Genetic research of six swamp eel (*Monopterus albus*) populations in the Yangtze River based on mitochondrial and microsatellite markers

Huaxing Zhou [Equal first author, 1], **Yuting Hu** [Equal first author, 1], **He Jiang** [Corresp., 1], **Guoqing Duan** [1], **Jun Ling** [1], **Tingshuang Pan** [1], **Xiaolei Chen** [1], **Huan Wang** [1]

[1] Anhui Key Laboratory of Aquaculture and Stock Enhancement, Fisheries Research Institution, Anhui Academy of Agricultural Sciences, Hefei, China

Corresponding Author: He Jiang
Email address: kenc7c7c7@126.com

The swamp eel (*Monopterus albus*) is a typical sex reversal fish with the high economic value. Several phylogeographic studies were performed based on various markers. However, the comparative research between different markers was still rare. In this study, the genetic structure of 180 individuals from six eel populations in the Yangtze River was explored based on two mitochondrial genes and ten microsatellite loci. The high diversity of six populations was revealed by genetic analyses. Significant differentiation of three tributary populations was detected and the habitat patch caused by seasonal cutoff was inferred as the main reason for this differentiation. Strong gene flow was detected among the mainstream populations which meant the distance was not the cause of isolation. Interestingly, the discordance occurred from the comparative analyses between two types of markers. The results of mitochondrial markers suggested genetic variation was mainly among populations and three tributary populations were highly differentiated. But the results of microsatellite markers suggested the variation was within populations and three tributary populations were moderately differentiated. We inferred this discordance mainly cause by incomplete inheritance of ancestral polymorphisms and the unique life history of sex reversal fish. Our study provided a new insight on the population genetic research of the sex reversal fish by the comparative analyses.

Genetic research of six swamp eel (*Monopterus albus*) populations in the Yangtze River based on mitochondrial and microsatellite markers

Huaxing Zhou[1①], Yuting Hu[1①], He Jiang[1✉], Guoqing Duan[1], Jun Ling[1], Tingshuang Pan[1], Xiaolei Chen[1], Huan Wang[1]

[1] Anhui Key Laboratory of Aquaculture and Stock Enhancement, Fisheries Research Institution, Anhui Academy of Agricultural Sciences, Hefei, China

✉: Corresponding author:
He Jiang
The Nongkenan road, Hefei, Anhui, 230031, China
Email address: kenc7c7c7@126.com

①: These authors contributed equally to this work

Abstract

The swamp eel (*Monopterus albus*) is a typical sex reversal fish with the high economic value. Several phylogeographic studies were performed based on various markers. However, the comparative research between different markers was still rare. In this study, the genetic structure of 180 individuals from six eel populations in the Yangtze River was explored based on two mitochondrial genes and ten microsatellite loci. The high diversity of six populations was revealed by genetic analyses. Significant differentiation of three tributary populations was detected and the habitat patch caused by seasonal cutoff was inferred as the main reason for this differentiation. Strong gene flow was detected among the mainstream populations which meant the distance was not the cause of isolation. Interestingly, the discordance occurred from the comparative analyses between two types of markers. The results of mitochondrial markers suggested genetic variation was mainly among populations and three tributary populations were highly differentiated. But the results of microsatellite markers suggested the variation was within populations and three tributary populations were moderately differentiated. We inferred this discordance mainly cause by incomplete inheritance of ancestral polymorphisms and the unique life history of sex reversal fish. Our study provided a new insight on the population genetic research of the sex reversal fish by the comparative analyses.

Keywords: *Monopterus albus*; Sex reversal; Population genetic research; Mitochondrial and nuclear markers

Introduction

The swamp eel (*Monopterus albus*) is a typical sex reversal fish, belongs to the family Synbranchidae, which usually inhabits in swamps, ponds and rice fields (Nelson et al., 2016). Due to its high nutritional and good taste, the swamp eel is used as a significant aquatic food in China. In 2018, 0.32 million tons of the swamp eel were produced by Chinese aquaculture (Fisheries Bureau of Ministry of Agriculture, 2019).

With the development of the eel farming, the population genetic research of the wild eel became a hot topic which guide the genetic breeding and eel culture. Several studies were explored by using different markers, such as microsatellites, mitochondrial genes, ISSR (Lei et al., 2012; Li et al., 2013; Liang et al., 2016). Li et al. (2013) compared the genetic diversity between wild and cultured swamp eel populations by ISSR markers. Liang et al. (2016) assessed the genetic structure of six eel populations in China. These researches provided important reference for eel breeding.

However, as the typical sex reversal fish, *Monopterus albus* has its unique life history (Liu, 1944; Qu, 2018). After spawning, the swamp eel is reversed from female to male. Due to the maternal inheritance of mitochondrial DNA, the genetic pattern of eel DNA is more complicated than normal fishes. Therefore, it is not preciseness enough to explore the population genetic structure of the sex reversal fish base on one single type of molecular markers.

In order to clarify the genetic variation under different longitudinal gradient, this study was performed in a small scale of the Yangtze River. Six populations, e.g., three mainstream populations and three tributary populations, were chosen along the Yangtze River and 180 individuals were collected. Subsequently, the genetic structure of these six populations was explored base on two mitochondrial genes and ten microsatellite loci. Here, the nuclear and mitochondrial genes were comparative analyzed. Different types of molecular markers will provide new insight on the population genetic research of the sex reversal fish.

Materials & Methods

67 **Ethics statement and Sample collection**

68 Procedures involving animals and their care were approved by the Animal Care and
69 Use Committee of Anhui Academy of Agricultural Sciences under approval number
70 201003076. Field experiments were approved by Fisheries Bureau of Anhui (project
71 number: FB/AH 2017-10).

72 180 eel individuals were collected from six populations in Anhui basin of the Yangtze
73 River (Tab. 1). DT, FC, HN were belong to the tributary of Yangtze River; WW, GC, WJ
74 were belong to the mainstream of Yangtze River (Fig. 1).

75 **DNA extraction and Marker genotyping**

76 Total genomic DNA was extracted from muscle tissue by a standard
77 phenol/chloroform procedure via proteinase K digestion (Sambrook et al., 1989), and then
78 kept at -20°C for PCR amplification.

79 The mitochondrial cytochrome c oxidase subunit I (*COI*) gene and cytochrome b (*Cyt*
80 *b*) gene were amplified with the designed primers. Ten unlinked polymorphic
81 microsatellite loci were selected from previous studies (Tab. S) (Lei et al., 2012; Li et al.,
82 2007; Zhuo et al., 2011).

83 PCR were conducted in 50 μL reaction mixtures containing 200 ng template DNA, 5
84 μL 10 × buffer (TaKaRa, Dalian, China), 4.0 μL $MgCl_2$ (2.5 mol/L), 3.0 μL dNTP (2.5 mM),
85 2 μL of each primer (5 μmol/L), and 0.5 U Taq DNA polymerase (25 U/μL, TaKaRa). PCR
86 conditions were as follows: initial denaturation (95°C, 1 min), then 35 cycles of
87 denaturation (94°C, 50 s), primer annealing (55°C, 45 s), and elongation (72°C, 1 min)
88 and a final extension (72°C, 10 min).

89 All PCR products were sequenced and genotyped by Sangon Biotech (Shanghai)
90 Co., Ltd.

91 **Data analyses**

92 Sequences were pretreated by DNASTAR Lasergene package. Subsequent
93 homologous alignment was performed by Mafft v.7 online program
94 (https://mafft.cbrc.jp/alignment/software/) (Katoh et al., 2017).

The haplotype diversity and nucleotide diversity were determined by DNAsp V.6 (Rozas et al., 2017). The analysis of molecular variance (AMOVA) were perform by Arlequin v.3.11 (Excoffier et al., 2005). Six populations were defined as a group. The inter-population and intra-population genetic variation were assessed. Pairwise F_{st} was estimated to evaluate the levels of population differentiation. The 5% significance levels were determined under 1×10^5 permutations. Subsequently, the number of individual migration (N_m) of each generation was calculated by F_{st} value (Slatkin and Barton, 1989).

The demographic history was explored by three approaches, e.g., neutral test, mismatch distribution and Bayesian Skyline Plots (BSP) analyses. Tajima's *D* (Tajima, 1989) and Fu's F_s (Fu, 1997) values reflected regulatory mutation by selection pressure. Mismatch distribution revealed the population dynamic variations (Rogers and Harpending, 1992). And the expansion time was calculated by the τ value with the equation τ=2μt, μ represented the nucleotide mutation rate, t represented the estimated expansion time. BSP analysis was performed by Beast v1.10.4 (Suchard et al., 2018) under uncorrelated relaxed clock mode for 5×10^7 generations.

Then a parsimony network was constructed for each haplotype using Median Joining (MJ) in NETWORK v.5.0. The genetic structure analysis was estimated using MCMC (Markov Chain Monte Carlo) algorithm as implemented in Structure v.2.3.3 (Hubisz et al., 2009). The number of clusters (K) was calculated under 1×10^6 generations with 10 replications. And the optimal number of K was deduced by Structure Harvester Web v.0.6.94 (Earl, 2012).

Results

Mitochondrial genes

A total of 1752 bp mitochondrial sequence (*COI* 665 bp, Accession number: MN097948 - MN098127; *Cyt b* 1087 bp, Accession number: MN098128 - MN098307) was obtained for analyses. The contents of the bases A, T, G and C were 24.6%, 29.3%, 14.6% and 31.5% respectively, which showed obvious anti-G bias (Saccone et al., 1999).

The 180 mitochondrial sequence corresponded to 86 distinct haplotypes (Tab. 2). All

haplotypes were divided into four clades based on MJ method (Fig. 2). Clade A was the largest one which contained five groups. Haplotype 5 (H-5) had the largest number of shared individuals, which was considered as the ancestral haplotype. The other three clades were separated by 13, 47, 24 mutational steps, respectively. Clade B only contained HN group. Clade C, D were mainly consisted of FC group and DT group, respectively. The populations of river tributary showed significant differentiation.

All six populations showed the high genetic diversity based on mitochondrial genes. Haplotype diversity was range from 0.6620 to 0.9793 and Nucleotide diversity was from 0.0017 to 0.0148 (Tab. 2). The result of AMOVA showed that genetic variation among populations (71.23%, $P < 0.001$) was much higher than the variation within the population (28.77%, $P < 0.001$) (Tab. 3a). Subsequent F_{st} and N_m values further confirmed this result. Strong gene flow was detected between the main steam populations (N_m = 20.1611 between GC and WW, N_m = 16.9825 between WJ and WW, N_m = 15.8934 between WJ and GC). And high differentiation was revealed between the tributary populations (F_{st} = 0.3069 - 0.9431) (Tab. 4a). The Fu's F_s and Tajima's D tests of mainstream populations were significant negative ($P<0.01$) which meant the expansion had occurred. No explicit expansion or decline were revealed for the tributary populations while the Fu's F_s and Tajima's D values were not significant (Tab. 5). The BSP analysis suggested the mainstream populations had suffered effective population size decline. Subsequent expansion time was estimated roughly as 0.46 MYA by the τ value. And three tributary populations maintain a relative constant population size (Fig. 3).

Microsatellite loci

Ten microsatellite loci amplified unambiguous and repeatable products in the size range expected. High genetic diversity was also revealed based on microsatellite data. The expected heterozygosity and observed heterozygosity of six populations were 0.8288 - 0.8876 and 0.5633 - 0.7200, respectively (Tab. 2).

Structure results suggested the highest posterior probability for K=4. The ΔK method revealed four potential genetic clusters which were respected by four colors, e.g., red,

yellow, green, purple. All populations contained multiple colors which meant the existence of inter-populations gene flow. And each population had a dominant genetic branch, e.g., DT was mainly dominated by the yellow cluster, FC was mainly composed by green cluster, HN was mainly contained the red cluster, the other three populations of mainstream were mainly dominated by the purple cluster (Fig. 4).

The AMOVA was performed based on the 10 microsatellite loci. The result suggested the genetic variation was mainly generated within populations (94.73%, $P < 0.001$) which was the opposite of the result based on mitochondrial data (Tab. 3b). F_{st} and N_m values suggested low level differentiation (F_{st} = 0.0052 - 0.0873) and the extensive gene flow (N_m = 2.6137 - 47.8269) between populations (Tab. 4b).

Discussion

Genetic structure of the six eel populations

All six populations revealed the high genetic diversity based on both mitochondrial and microsatellite markers. The genetic diversity level of this study was higher than Liang's results (*Hd* = 0.708, *Pi* = 0.002) (Liang et al., 2016). The genetic diversity of FC population was the lowest. No significant difference in the level of genetic diversity was detected between the tributary and mainstream populations.

The significant differentiation of three tributary populations was revealed by the population genetic analyses. Haplotype network and structure results suggested the tributary populations formed three separate clades which contained their unique genetic lineages. We inferred the habitat patch caused by seasonal cutoff was the main reason for this differentiation. Interestingly, strong gene flow was detected among the mainstream populations. And the expansion of mainstream populations was detected. It is well known that the swamp eel is the cave fish whose fins are vestigial or absent. Compared with common fish, the movement ability of eel is weak. Thus, we were curious about the reasons for this long-distance gene flow. Similar situations of other species had been reported (Cure et al., 2017; Zhou et al., 2015). The trade was considered to be the major factor for gene flow. Besides, the rapid flow of mainstream also provided the

conditions for the long-distance gene flow.

Comparative analyses between mitochondrial and microsatellite data

The discordance occurred in tributary population structure based on different molecular markers. Based on mitochondrial genes, the genetic variation was mainly generated among populations. All tributary populations were highly differentiated (F_{st} > 0.25) and gathered three monophyletic clades. However, the genetic variation was mainly generated within populations based on microsatellite data. And three tributary populations were moderately differentiated (0.05 < F_{st} < 0.15). The mean F_{st} values of tributary populations based on mitochondrial genes and microsatellite data were 0.6777 and 0.0631, respectively. Considering the different mutation rates, the mitochondrial F_{st} was corrected by the equation, F_{st} (nuc) = F_{st} (mt)/[4–3 F_{st} (mt)] (Brito, 2007), in order to reduce the differentiation between mtDNA and nDNA. Even so, corrected mitochondrial F_{st} value was still ten times higher than the F_{st} estimated with microsatellite data. However, the mean F_{st} values of mainstream populations based on mitochondrial genes and microsatellite data were 0.0278 and 0.0082, respectively. After correction, the two values were almost equal.

Our studies provided an interesting pattern that the discordance occurred in tributary population structure based on different molecular markers while the results of mainstream populations were consistent. According to previous studies, sex-biased dispersal, genetic admixture and incomplete inheritance of ancestral polymorphisms may be the potential reasons for the discordance caused by different molecular markers (Funk and Omland, 2003; Qu et al., 2012; Yang et al., 2016; Zarza et al., 2011). This study, the historical demographic analyses suggested mainstream populations had expanded after effective population size decline and three tributary populations maintain a relative constant population size. The expansion of the mainstream populations has led to a high level of gene flow. And the isolation among the tributary populations may the external factor for this discordance. Thus, we suggested the incomplete inheritance of ancestral polymorphisms may account for the discordant based on different molecular markers in

swamp eels.

Considering the sex reversal, we inferred the unique life history of the swamp eel also contributed to this discordant. Initially, the swamp eel spawns as female which can provide both mitochondrial and nuclear DNA to the population genetic pool. After spawning, the swamp eel is reversed from female to male. Then, the swamp eel as male only provides nuclear DNA to the population genetic pool by the sperm (Fig. 5). The egg number of swamp eel is much lower than common fishes which meant the eel was suffered greater genetic drift risk (Duan et al., 2016). The survival rate of seedlings and eggs was low while selective pressure regulated. After sex reversed, the mitochondrial genetic information was likely lost under the genetic drift (Nei et al., 1975). Thus, different genetic frequencies between mitochondrial and nuclear genes in isolation populations may cause the discordance.

Conclusions

Our study used two data sets, mitochondrial DNA and microsatellites, to explore the demographic genetic variation of swamp eels. The high genetic diversity suggested that the resource of swamp eel in Anhui basin was abundant and had the potential breeding value. Each tributary population should be treated as the independent genetic unit. The incomplete inheritance of ancestral polymorphisms and the sex reversal life history of the swamp eel may be the significant factors affecting the population genetic structure and generate the discordance based on different molecular markers. Finally, although further research is needed, our study still provided a novel insight on the population genetic research of the sex reversal fish.

References

Brito PH. 2007. Contrasting patterns of mitochondrial and microsatellite genetic structure among Western European populations of tawny owls (*Strix aluco*). *Molecular ecology* 16: 3423-3437

Cure K, Thomas L, Hobbs J-PA, Fairclough DV, Kennington WJ. 2017. Genomic signatures of local adaptation reveal source-sink dynamics in a high gene flow fish species. *Scientific reports* 7: 8618

Duan G, Jiang H, Hu W, Pan T, Hu Y, Ling J. 2016. The Comparison of Individual Fecundity of *Monopterus albus* from Different Sources. *Progress in Fishery Sciences* 37: 84-90

Earl DA. 2012. STRUCTURE HARVESTER: a website and program for visualizing STRUCTURE output and implementing the Evanno method. *Conservation genetics resources* 4: 359-361

Excoffier L, Laval G, Schneider S. 2005. Arlequin (version 3.0): an integrated software package for population genetics data analysis. *Evolutionary bioinformatics* 1: 47-50

Fu YX. 1997. Statistical tests of neutrality of mutations against population growth, hitchhiking and background selection. *Genetics* 147: 915-925

Funk DJ, Omland KE. 2003. Species-level paraphyly and polyphyly: frequency, causes, and consequences, with insights from animal mitochondrial DNA. *Annual Review of Ecology, Evolution, and Systematics* 34: 397-423

Hubisz MJ, Falush D, Stephens M, Pritchard JK. 2009. Inferring weak population structure with the assistance of sample group information. *Molecular ecology resources* 9: 1322-1332

Katoh K, Rozewicki J, Yamada KD. 2017. MAFFT online service: multiple sequence alignment, interactive sequence choice and visualization. *Briefings in bioinformatics*

Lei L, Feng L, Jian TR, Yue GH. 2012. Characterization and multiplex genotyping of novel microsatellites from Asian swamp eel, *Monopterus albus*. *Conservation genetics resources* 4: 363-365

Li W, Liao X, Yu X, Cheng L, Tong J. 2007. Isolation and characterization of polymorphic microsatellites in a sex-reversal fish, rice field eel (*Monopterus albus*). *Molecular ecology notes* 7: 705-707

Li W, Sun WX, Fan J, Zhang CC. 2013. Genetic diversity of wild and cultured swamp eel (*Monopterus albus*) populations from central China revealed by ISSR markers. *Biologia* 68: 727-732

Liang H, Guo S, Li Z, Luo X, Zou G. 2016. Assessment of genetic diversity and population structure of swamp eel *Monopterus albus* in China. *Biochemical systematics and ecology* 68: 81-87

Liu CK. 1944. Rudimentary hermaphroditism in the symbranchoid eel, *Monopterus favanensis*. *Sinensia* 15: 1-18

Nei M, Maruyama T, Chakraborty R. 1975. The bottleneck effect and genetic variability in populations. *Evolution* 29: 1-10

Nelson JS, Grande TC, Wilson MV. 2016. Fishes of the world. John Wiley & Sons Press

Qu XC. 2018. Sex determination and control in eels. In: *Sex Control in Aquaculture*. John Wiley & Sons Press. 775-792

Qu Y, Zhang R, Quan Q, Song G, Li SH, Lei F. 2012. Incomplete lineage sorting or secondary admixture: disentangling historical divergence from recent gene flow in the V inous-throated parrotbill (*Paradoxornis webbianus*). *Molecular ecology* 21: 6117-6133

Rogers AR, Harpending H. 1992. Population growth makes waves in the distribution of pairwise genetic differences. *Molecular biology and evolution* 9: 552-569

Rozas J, Ferrer-Mata A, Sánchez-DelBarrio JC, Guirao-Rico S, Librado P, Ramos-Onsins SE, Sánchez-Gracia A. 2017. DnaSP 6: DNA sequence polymorphism analysis of large data sets. *Molecular biology and evolution* 34: 3299-3302

Saccone C, De Giorgi C, Gissi C, Pesole G, Reyes A. 1999. Evolutionary genomics in Metazoa: the mitochondrial DNA as a model system. *Gene* 238: 195-209

Sambrook J, Fritsch EF, Maniatis T. 1989. *Molecular cloning: a laboratory manual*. Cold

286 spring harbor laboratory press
287 Slatkin M, Barton NH. 1989. A comparison of three indirect methods for estimating
288 average levels of gene flow. *Evolution* 43: 1349-1368
289 Suchard MA, Lemey P, Baele G, Ayres DL, Drummond AJ, Rambaut A. 2018. Bayesian
290 phylogenetic and phylodynamic data integration using BEAST 1.10. *Virus Evolution*
291 4: vey016
292 Tajima F. 1989. Statistical method for testing the neutral mutation hypothesis by DNA
293 polymorphism. *Genetics* 123: 585-595
294 Yang JQ, Hsu KC, Liu ZZ, Su LW, Kuo PH., Tang WQ, Zhou ZC, Liu D, Bao BL, Lin HD.
295 2016. The population history of *Garra orientalis* (Teleostei: Cyprinidae) using
296 mitochondrial DNA and microsatellite data with approximate Bayesian computation.
297 *BMC evolutionary biology* 16: 73
298 Zarza E, Reynoso VH, Emerson BC. 2011. Discordant patterns of geographic variation
299 between mitochondrial and microsatellite markers in the Mexican black iguana
300 (*Ctenosaura pectinata*) in a contact zone. *Journal of Biogeography* 38: 1394-1405
301 Zhou H, Jiang Y, Nie L, Yin H, Li H, Dong X, Zhao F, Zhang H, Pu Y, Huang Z. 2015. The
302 historical speciation of *Mauremys* Sensu Lato: ancestral area reconstruction and
303 interspecific gene flow level assessment provide new insights. *PloS one* 10:
304 e0144711
305 Zhuo Y, Hu H, Zhang L, Shu M. 2011. Microsatellite analysis of genetic diversity of
306 *Monopterus albus* along the middle and lower reaches of Yangtze River basin.
307 *Biotechnology Bulletin* 11: 187-192

Table 1(on next page)

Sampling information of *Monopterus albus*

1 **Table 1. Sampling information of *Monopterus albus***

Populations	Sampling basin	Sampling number	Sampling coordinates	
			Longitude	Latitude
DT	The tributary of Yangtze River	30	118.62	31.52
WW	The mainstream of Yangtze River	30	117.98	31.16
FC	The tributary of Yangtze River	30	118.24	31.11
GC	The mainstream of Yangtze River	30	117.65	30.76
HN	The tributary of Yangtze River	30	117.03	30.75
WJ	The mainstream of Yangtze River	30	116.89	30.35

2

Table 2(on next page)

Genetic diversity of 6 populations of *Monopterus albus*

Hd represents Haplotype diversity, *Pi* represents Nucleotide diversity, *He* represents Expected heterozygosity; *Ho* represents observed heterozygosity

Table 2. Genetic diversity of 6 populations of *Monopterus albus*

populations	Mitochondrial genes			Microsatellite loci		
	Num. of haplotypes	*Hd*	*Pi*	Num. of alleles	*He*	Ho
DT	18	0.9540	0.0148	15	0.8876	0.7200
WW	24	0.9793	0.0078	16	0.8826	0.6733
FC	9	0.6620	0.0017	13	0.8288	0.5933
GC	15	0.8480	0.0021	14	0.8602	0.6667
HN	13	0.9220	0.0072	13	0.8292	0.5633
WJ	19	0.9240	0.0023	16	0.8781	0.7138

***Hd* represents Haplotype diversity, *Pi* represents Nucleotide diversity, *He* represents Expected heterozygosity; *Ho* represents observed heterozygosity**

Table 3(on next page)

AMOVA of 6 populations of *Monopterus albus*

Table 3a. AMOVA of 6 populations of *Monopterus albus* based on mt genes

Source of variation	d*f*	Sum of squares	Percentage of variation	*P* value
Among population	5	1965.433	71.23	<0.001
Within population	174	908.533	28.77	<0.001
Total	179	2873.967		

Table 3b. AMOVA of 6 populations of *Monopterus albus* based on microsatellite loci

Source of variation	d*f*	Sum of squares	Percentage of variation	*P* value
Among population	5	92.999	5.27	<0.001
Within population	352	1515.342	94.73	<0.001
total	357	1608.341		

Table 4(on next page)

Pairwise values of F_{st} (below diaonal) and N_m (above diagonal) between populations

Table 4a. Pairwise values of F_{st} (below diaonal) and N_m (above diagonal) between populations based on mt genes

	DT	WW	FC	GC	HN	WJ
DT		0.3028**	0.3621**	0.1853**	0.2763**	0.1894**
WW	0.6228**		0.0875**	20.1611	1.1292**	16.9825
FC	0.5800**	0.8510**		0.0302**	0.0847**	0.0324**
GC	0.7296**	0.0242	0.9431**		0.5526**	15.8934**
HN	0.6441**	0.3069**	0.8551**	0.4750**		0.5884**
WJ	0.7253**	0.0286	0.9391**	0.0305**	0.4594**	

*** P<0.05; **P<0.01; N_m=0.5×(1- F_{st})/ F_{st}**

Table 4b. Pairwise values of F_{st} (below diaonal) and N_m (above diagonal) between populations based on microsatellite loci

	DT	WW	FC	GC	HN	WJ
DT		4.1360**	3.0656**	3.2271**	2.6137**	3.8754**
WW	0.0570**		4.7400**	18.8340*	4.2626**	39.4325
FC	0.0754**	0.0501**		3.8959**	2.8517**	4.8313**
GC	0.0719**	0.0131*	0.0603**		3.7888**	47.8269
HN	0.0873**	0.0554**	0.0806**	0.0619**		5.0805**
WJ	0.0606**	0.0063	0.0492**	0.0052	0.0469**	

*** P<0.05; **P<0.01; N_m=0.25×(1- F_{st})/ F_{st}**

Table 5(on next page)

Neutral test and mismatch distribution of 6 populations of *Monopterus albus*

* $P<0.05$; ** $P<0.01$

1 **Table 5. Neutral test and mismatch distribution of 6 populations of *Monopterus albus***

Populations	Tajima's *D*	Fu's F_s	τ	θ_0	θ_1
Mainstream populations	-2.3328**	-24.9078**	2.2949	1.5484	20.4492
DT	0.6878	1.8735	0.3906	9.9826	99999.0
FC	-2.4163**	-0.8094	0.375	0.0	99999.0
HN	0.4788	2.1653	22.5293	0.0018	27.6941

2 *** *P*<0.05; ***P*<0.01**

3

Figure 1

Sampling sites of six eel populations using DIVA-GIS.

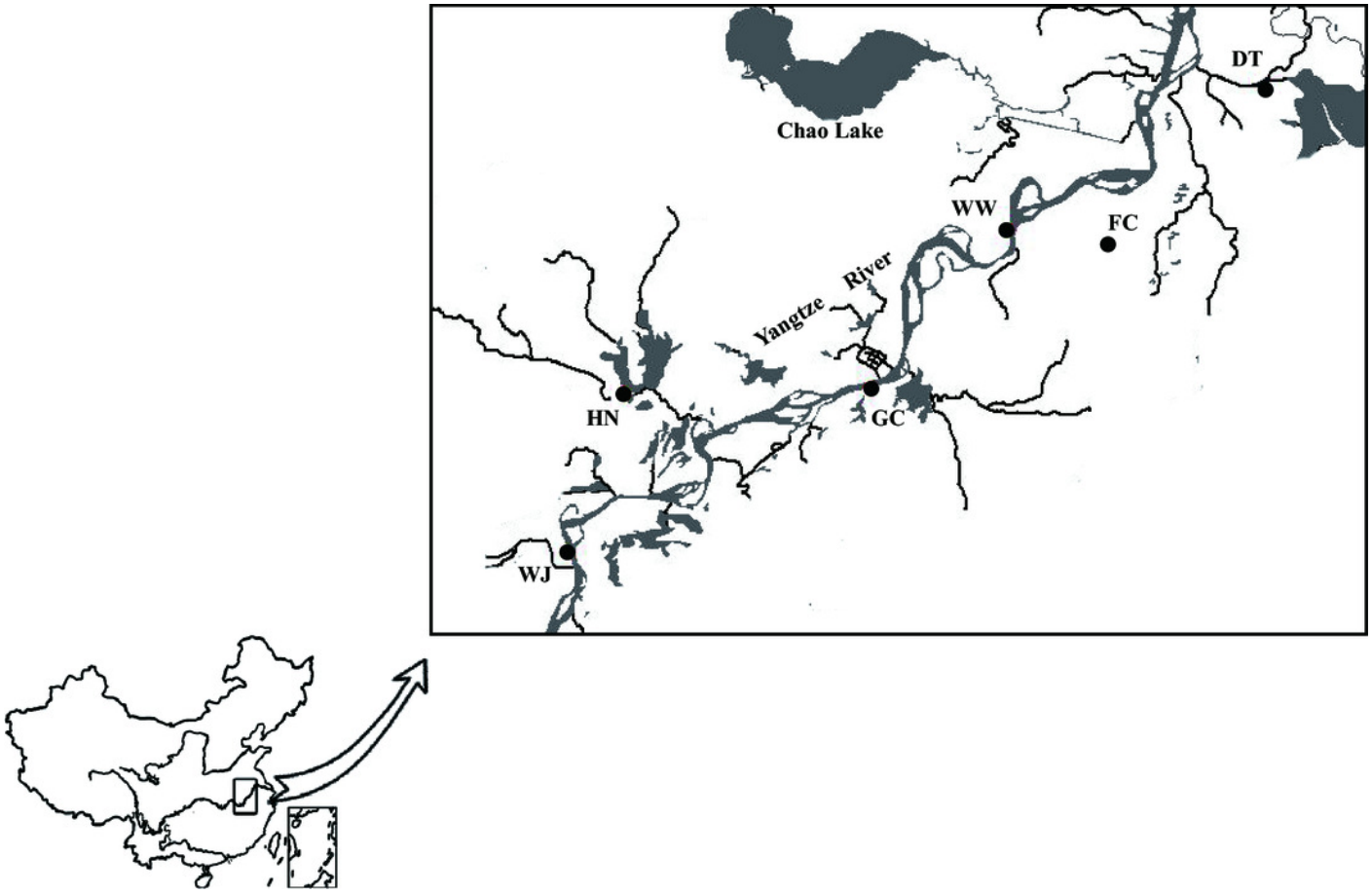

Figure 2

Haplotype network based on MJ methods.

Different colors represent the six populations. Circle size represents the number of species and numbers of nearby branches represent the mutation steps.

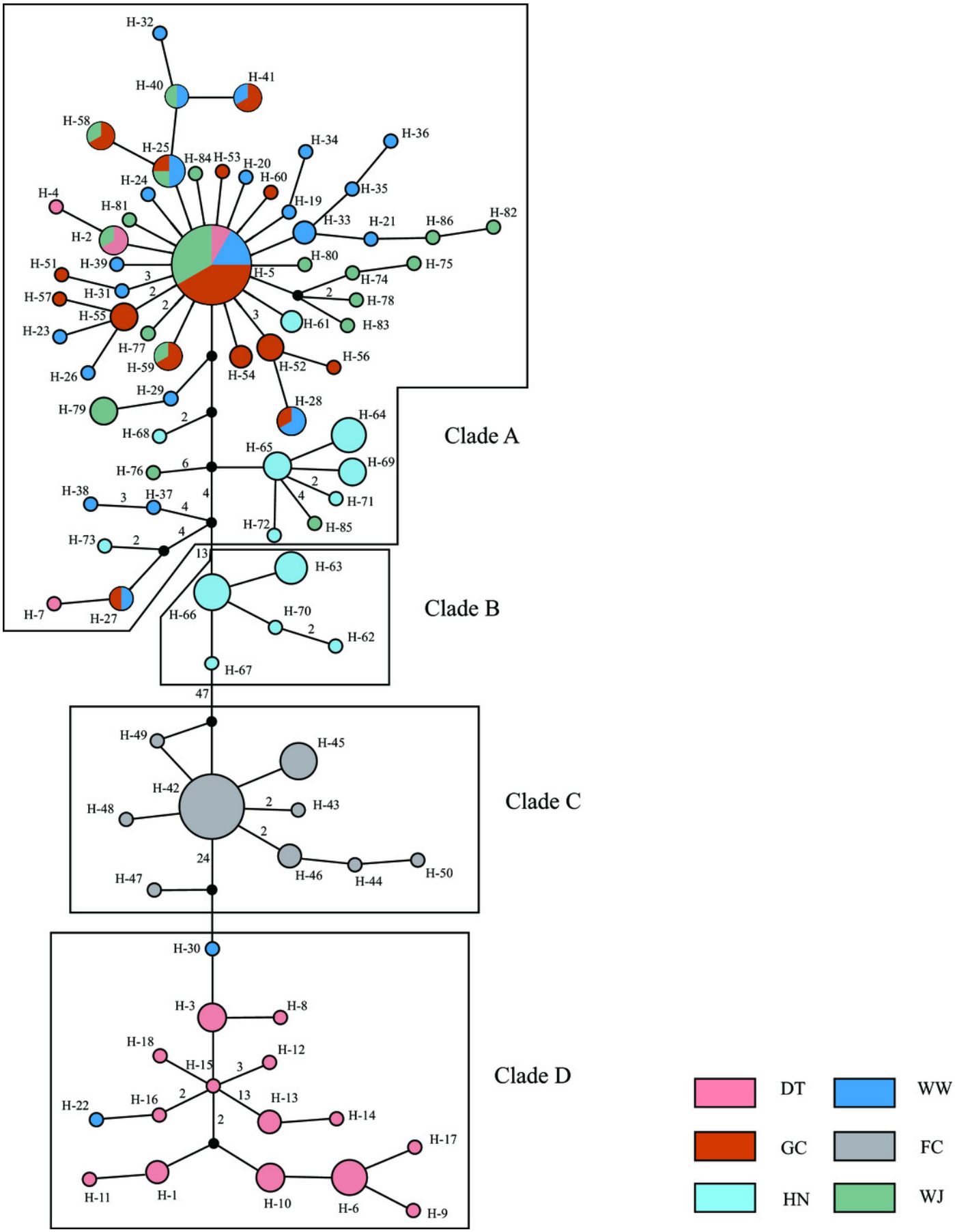
H-32
H-40
H-41
H-58
H-25
H-84
H-53
H-20
H-60
H-34
H-36
H-24
H-35
H-4
H-81
H-19
H-33
H-21
H-86
H-82
H-2
H-80
H-75
H-51
H-39
H-5
H-74
H-57
H-31
H-78
H-55
H-61
H-83
H-23
H-77
H-59
H-54
H-52
H-56
H-26
H-29
H-28
H-79
H-64
H-68
H-65
H-69
H-76
H-71
H-38
H-37
H-72
H-85
H-73
H-63
H-7
H-27
H-66
H-70
H-62
H-67
H-49
H-45
H-42
H-48
H-43
H-46
H-44
H-50
H-47
H-30
H-3
H-8
H-18
H-12
H-15
H-22
H-16
H-13
H-14
H-17
H-11
H-1
H-10
H-6
H-9
Clade A
Clade B
Clade C
Clade D
DT
WW
GC
FC
HN
WJ

Figure 3

The demographic history inferred from *COI* and *Cyt b* genes.

Three mainstream populations were treat as one group. A: Mismatch distribution; B: Bayesian skyline plots, the shaded area represents the 95% confidence intervals of HPD analysis.

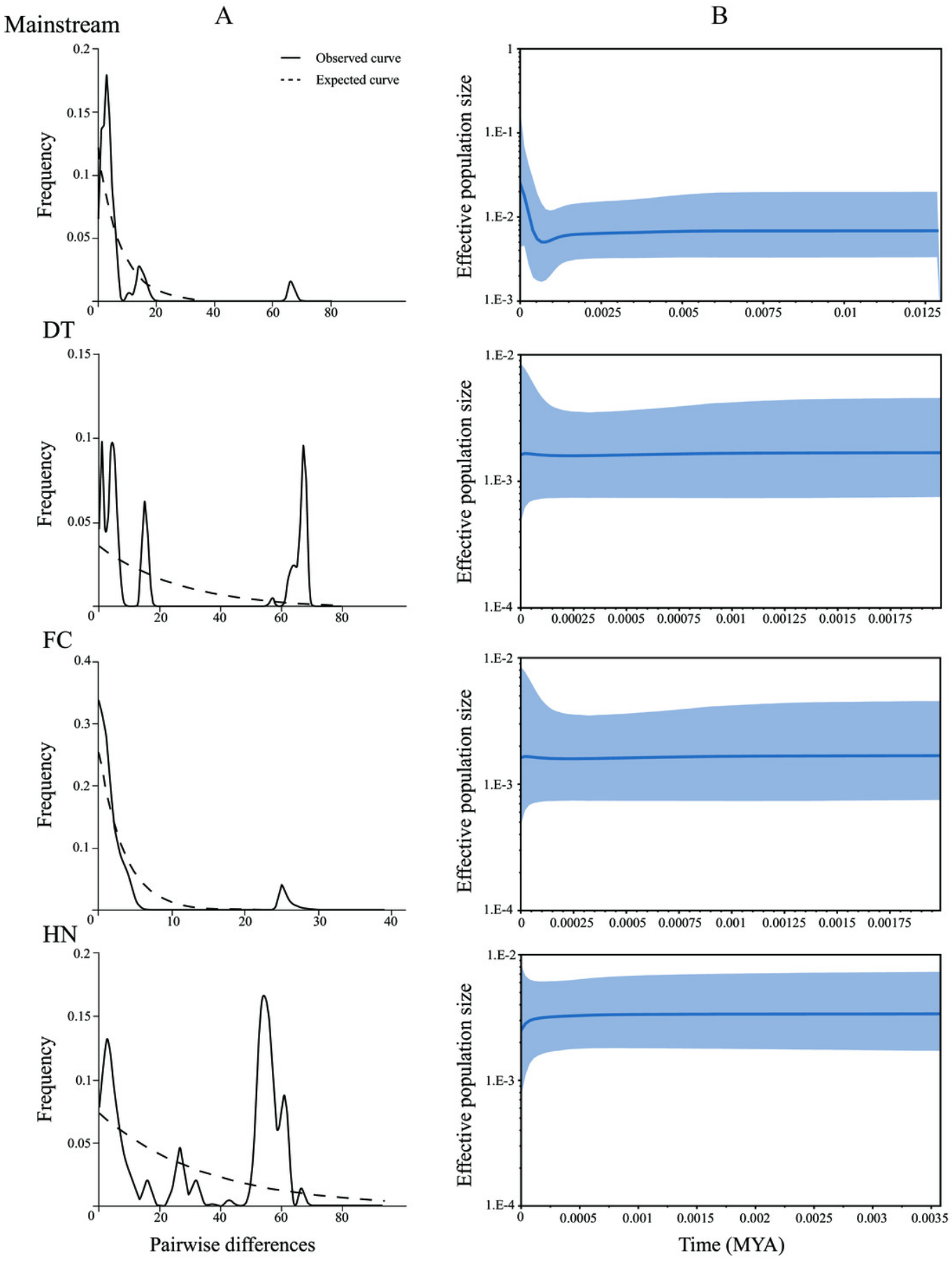
A
B
Mainstream
Observed curve
Expected curve
Frequency
Effective population size
DT
FC
HN
Pairwise differences
Time (MYA)

Figure 4

Population structure of 180 swamp eels for K = 4.

Four colors, e.g., red, yellow, purple and green, represent the inferred gentic clusters.

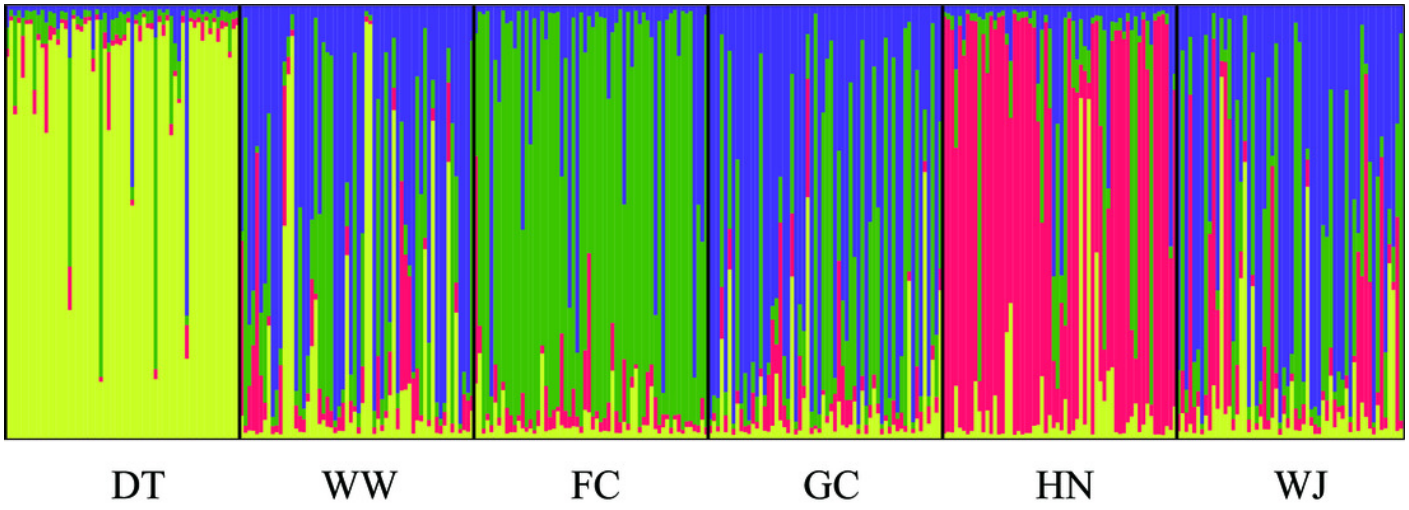

Figure 5

Different hereditary patterns of mitochondrial DNA and nuclear DNA in sex reversal fish.